BUTTERWORTH HEINEMANN

Polymer Vol. 36 No. 16, pp. 3113–3126, 1995

0032-3861/95/$10.00+0.00

In situ reinforcement of polypropylene with liquid-crystalline polymers: effect of maleic anhydride-grafted polypropylene

Hugh J. O'Donnell* and Donald G. Baird†
Polymer Materials and Interfaces Laboratory, and Department of Chemical Engineering, Virginia Polytechnic Institute and State University, Blacksburg, VA 24061, USA
(Received 18 September 1994; revised 27 February 1995)

The effect of maleic anhydride-grafted polypropylene (MAP) on the mechanical properties of three polypropylene/liquid-crystalline polymer (PP/LCP) blends was investigated. Three LCPs were used in the study. One LCP was a poly(ester amide) and the other two LCPs were copolyesters. The tensile properties of the PP/liquid-crystal (LC) poly(ester amide) blend were affected by the addition of MAP to a greater extent than were the tensile properties of the two PP/LC copolyester blends. The tensile strength of the former blend increased without reaching a plateau as the level of MAP was increased, whereas the tensile strength of the latter blends showed that a plateau or maximum in the strength existed. The tensile modulus of the PP/LC poly(ester amide) blend showed a 19% increase as the amount of MAP was increased above 5 wt%. Only small changes occurred in the modulus of the PP/LC copolyester blends. The effect of MAP on the mechanical properties of PP/LCP blends indicated that MAP interacted with the amide group preferentially over the ester group. An excess of MAP was also shown to change the morphology from larger elongated structures to smaller structures that can lead to reduced tensile moduli. Measurement of the contact angles of liquids on PP, PP/MAP and the three LCPs indicated that MAP lowered the interfacial tension for all three PP/LCP blends. The reduced interfacial tension and increased adhesion indicated that MAP compatibilized the PP/LCP blends. While in most polymer blends compatibilization leads to finely dispersed drops of the minor components, LCP fibrils were obtained over a large range of compatibilizer concentrations. Finally, isolation of the PP/MAP phase from the LCP phase indicated that MAP did not react with the LCP. Instead, an interaction such as hydrogen bonding was believed to be responsible for the compatibilizing effect of MAP on PP/LCP blends.

(Keywords: polypropylene; liquid-crystalline polymers; *in situ* composites)

INTRODUCTION

A frequent goal of polymeric material research is the improvement of physical properties. An approach that is widely used is the combination of two polymers in the hope of obtaining favourable properties in the blend. If successful, this route can lead to the creation of attractive new composite materials. One relatively new type of blend is that of thermotropic liquid-crystalline polymers (LCPs) and thermoplastic (TP) matrices. Neat LCPs exhibit very high mechanical properties as a result of their stiff molecular backbones[1], their relative ease to orient and their ability to retain this orientation for up to several minutes in the melt state[2,3]. Commercially available LCP resins processed by means of injection moulding have moduli in the range from 4 to 20 GPa and strengths from 139 to 213 MPa[4]. In comparison, injection-moulded thermoplastic resins have much lower properties, with moduli typically in the range of 1 to 4 GPa and strengths from 20 to 60 MPa[5]. A key for reinforcement of TP matrices with LCPs is the creation of LCP fibrils by use of appropriate processing conditions. These fibrils serve to reinforce the matrix in an analogous manner to fibre-reinforced composites. As a result of this similarity, LCP-reinforced TP are often termed *in situ* composites.

Several key factors affect the ability of LCPs to reinforce thermoplastics. The first factor is the influence of the flow field on orientation and mechanical properties of neat LCPs. A uniaxial extensional flow field is very effective in bringing about molecular orientation within neat LCPs[6–11]. Ide and Ophir[7] demonstrated this point by varying the draw ratio and shear rate during capillary extrusion of an LCP. Both the orientation and moduli of these samples were significantly improved by drawing the extrudate. Conversely, increasing the shear rate within the die decreased the moduli.

While the type of flow field is important in creating orientation in neat LCPs, it also plays an important role when the LCP is the dispersed phase of a polymer blend. In polymer blends, the deformation of the LCP phase occurs most readily in an extensional flow field such as uniaxial extensional flow to form fibrils with high aspect ratios. These fibrils can create effective reinforcement of

*The Procter and Gamble Company, Winton Hill Technical Center, 6110 Center Hill Ave., Cincinnati, OH 45224, USA
† To whom correspondence should be addressed

the matrix, leading to high mechanical properties[12–16]. However, once the fibrils are formed, they must be solidified before interfacial instabilities occur, which would lead to break-up of the fibres into droplets[17,18], or before undergoing relaxation, which would cause a significant loss in their molecular orientation[2,3].

The concentration of an LCP within a matrix and the flow geometry have also been shown to be critical factors in creation of a fibrous morphology[13–15]. Blizard and Baird[15] demonstrated this point with blends of an LCP based on poly(ethylene terephthalate)/*p*-hydroxybenzoic acid (PET/PHB) with polycarbonate (PC) or nylon-6,6 matrices. Blends with 10 wt% LCP extruded through a capillary die with a small L/D ratio of 7 were found to have a droplet morphology. However, fibrils were obtained when the concentration reached 30% LCP. An increased dispersed phase size created by an increased rate of coalescence at the higher LCP concentration was believed to be responsible for the formation of fibres at 30 wt% LCP. In a die with larger L/D ratio of 27 a droplet morphology was found at both concentrations. The change from a smaller to greater L/D ratio is accompanied by an increased residence time in the die. While fibres may have been formed at the entrance to the die, the increased time under shear flow in the longer die allows interfacial forces to break the fibres into droplets. From this study, it can be stated that the existence of extensional flows and higher concentrations are important factors that can lead to the creation of a reinforcing morphology.

Even when extensional flows and higher concentrations exist, this may not be sufficient for obtaining a reinforcing morphology. The temperature range required for processing each material must suitably overlap. Typically, LCPs are processed above 300°C while thermoplastics are processed below this temperature. Despite this temperature difference, a fibrous morphology with enhanced mechanical properties can often be created within many TP/LCP blends. However, some exceptions do exist[14,19,20]. For instance, in the drawing of extruded strands of K161, a proprietary LCP from the Bayer Co., in a poly(ether imide) (PEI) matrix, Carfagna *et al.*[19] found little improvement in the mechanical properties as the draw ratio was increased. The limited effect of draw ratio on the mechanical properties was related to the large differences between the glass transition temperatures of the two materials[19]. Blizard *et al.*[20] found similar results for the drawing of blends of LCPs with PC and PEI matrices.

While high temperatures are generally required to process TP/LCP blends, temperatures much higher than the melting point of the LCP may lead to a reduction in the mechanical properties of the blend. Nobile *et al.*[14] found that the morphology and the mechanical properties of drawn strands of 10 wt% PET/PHB in a PC matrix were sensitive to temperature. At 260°C, a droplet morphology was observed, while at 220°C, a fibrillar morphology was observed. Correspondingly, lower properties were measured for the blend processed at 260°C than for the blend processed at 220°C. The improved properties at a lower processing temperature may be the result of at least two factors. The first factor is that higher hydrodynamic stresses at the lower temperature lead to a higher Weber number, which would provide the conditions needed to deform smaller LCP droplets. The second factor is that the lower temperature may result in improved retention of molecular orientation or may permit solidification of the elongated LCP structures before interfacial tension can cause break-up or retraction of the elongated structures.

While the above factors significantly affect the ability of LCPs to reinforce TPs, the degree of miscibility of a TP/LCP pair can also have a marked influence on the resulting properties. For several TP/LCP blends studied by Zhuang *et al.*[21], it was found that partially miscible systems exhibited the highest strengths while totally immiscible systems displayed strengths that did not differ significantly from the strength of the matrix. In an attempt to predict suitable polymer pairs, Meretz[22] proposed selecting pairs based on the interfacial tension and polarity differences as calculated from contact-angle measurements on neat solid samples. Unfortunately, the mechanical properties for only one pair were investigated, thus leaving open the question as to the accuracy of this method for predicting properties of a wide range of polymer pairs.

While polymer pairs that lead to enhanced mechanical properties are desired, the mechanical properties of two less suitable polymers might be enhanced by the use of a third interfacially active component. The process of bringing about enhanced mechanical properties by the addition of a minor third component is termed compatibilization[23,24]. Compatibilization is often used in a thermoplastic blend to enhance the toughness and the impact strength of the matrix by adding a rubbery phase. Without compatibilizer, the blend components would exhibit poor adhesion and large phase sizes, and the blend would exhibit poor mechanical properties. The compatibilizer may be a copolymer consisting of two blocks that are similar to the polymers in the blend, blocks capable of creating specific interactions with the polymers, or a functionalization of one of the polymers so that it is capable of undergoing a graft reaction with the dissimilar polymer. Reviews of compatibilizer types and reports of successful uses of compatibilizers may be found elsewhere[23–25]. A common point in these reviews is that successful compatibilization can be characterized by three features: reduced interfacial tension, finer dispersions and increased adhesion. In addition, successful compatibilization results in mechanical property improvements. In particular, the impact strength and toughness of TP blends are markedly improved.

While the use of compatibilizers with TP blends is widespread, in only one case has there been a report of compatibilized TP/LCP blends: the blend of polypropylene (PP) with various LCPs[26–30]. Because of the incompatible nature of PP with the LCPs, a third polymer, maleic anhydride-grafted PP (MAP), was added in an attempt to improve the adhesion between the phases and enhance the mechanical properties of the blend. However, as noted above for thermoplastic blends, a compatibilizer creates a droplet morphology, which leads to lower tensile properties. For a compatibilizer to aid the reinforcement of TP by LCPs, the compatibilizer must not cause the loss of the fibrous morphology that typifies *in situ* composites, and it must improve the adhesion between phases. Examination of the compatibilized PP/LCP blends reveals a more finely dispersed fibrillar structure than is observed in uncompatibilized blends, and the tensile strength and modulus of the

compatibilized blends are enhanced over those of uncompatibilized PP/LCP blends[26–29]. Additionally, a greatly reduced degree of fibre pull-out occurs, which indicates that adhesion does indeed improve[26]. Hence, although MAP appears to function in a manner similar to that observed for flexible-chain polymer blends, it should be noted that in a TP/LCP blend the use of MAP leads to a fibrillar morphology and improved tensile properties, which differs from the changes brought about through compatibilization of TP blends.

There are still several unanswered questions remaining as to the effect of MAP on the mechanical properties of PP/LCP blends. The first question pertains to the effect of the amount of MAP on the mechanical properties of the blends. In particular, do the properties reach a plateau as the concentration of MAP increases? Secondly, will the use of increasing amounts of MAP lead to a morphological change from a fibrillar to a droplet morphology? Such a morphological change would lead to a change in the aspect ratio and, consequently, to a decline in the modulus as predicted for fibre-reinforced composites[31]. Thirdly, can the changes at the interface be measured or indirectly obtained, and if so does the compatibilizer lower the interfacial tension and enhance adhesion? Finally, does MAP compatibilize these blends through a physical interaction or via a chemical reaction? Knowledge of the type of interaction may be helpful in a search for other, possibly even more effective, compatibilizers.

To pursue the answers to these questions, the effect of increasing concentration of MAP on the mechanical properties of PP/LCP blends with a fixed LCP percentage, 30 wt%, is investigated. The objective of this work is threefold. The first objective is to determine to what extent the concentration of MAP affects the mechanical properties of the blend. The second objective is to determine if the presence of MAP leads to reduced interfacial tension and enhanced adhesion between the phases. The final objective is to determine if the compatibilization effect of MAP is the result of physical interaction or chemical reaction.

EXPERIMENTAL

Materials

Five polymers were used in this work. The polypropylene (Profax 6823) was a fractional melt flow index (*MFI*) polymer purchased from Himont Inc. The compatibilizer was a development-grade maleic anhydride-grafted polypropylene (MAP) supplied by Uniroyal Inc., with a *MFI* of 50. This material was titrated as outlined elsewhere[27] and found to have 0.75 wt% maleic anhydride. Three LCPs were used in this study. Two were copolyesters and the other was a poly(ester amide). The first LCP was Vectra® A950 purchased from Hoechst Celanese, and hereafter referred to as VA. This polymer was reportedly synthesized from the following monomers: 73% hydroxybenzoic acid and 27% hydroxynaphthoic acid. The second LCP was Vectra B950 (VB) purchased from Hoechst Celanese. This polymer was reportedly synthesized from 60% hydroxynaphthoic acid, 20% terephthalic acid and 20% aminophenol. The latter ingredient created the amide moiety within the LCP, which was incorporated to increase hydrogen bonding with other polymers[32]. The third LCP was LC3000 supplied by Unitika, Japan. This polymer was based on 40% poly(ethylene terephthalate) copolymerized with 60% hydroxybenzoic acid.

Sample preparation

All blends containing MAP were first prepared by mixing PP with MAP in a one inch (~ 25 mm), $L/D = 24$, Killion extruder at 40 r.p.m. and 250°C. The residence time in the extruder was approximately 90 s. This material is the matrix, and it will be designated as PP(MAP) throughout this paper. All injection-moulded specimens were prepared on an Arburg Allrounder (model 221-55-250) injection moulder. Both tensile bars and plaques were produced. The tensile bars were 63.5 mm × 9.5 mm × 1.5 mm and the width at the neck was 3.2 mm (ASTM D638 type V bars). The plaques were 76 mm × 76 mm × 1.5 mm. This plaque mould was machined with a film gate to provide two-dimensional rectilinear flow throughout the cavity.

The blends were prepared by tumbling dried pellets of PP(MAP) with dried pellets of the appropriate LCP immediately before use in the injection moulder. PP(MAP) and LCP were dried overnight in a vacuum oven and convection oven, respectively. Both VA and VB blends were moulded with the three barrel zone temperatures set to 160, 295 and 295°C, the nozzle temperature set to 280°C and the mould temperature set to 40°C. Blends of LC3000 were moulded with the three barrel zone temperatures set to 160, 265 and 265°C, the nozzle temperature set to 250°C and the mould temperature set to 40°C. Injection moulding filling and cooling times were 1.5 and 15 s, respectively.

The blend compositions were designated in a special manner. An example will best illustrate this designation. If a PP(MAP) matrix containing 10 wt% MAP is blended with an LCP so that 30 wt% LCP results, then this blend will be labelled as PP(MAP)/LCP 70(10)/30. The first number, 70, indicates the weight percentage of PP(MAP) within the blend and the second number, 10, indicates the weight percentage of MAP within the PP(MAP) phase. The last number indicates the weight percentage of LCP in the blend. This method of designation was convenient to use since PP(MAP) matrices were prepared prior to blending with the LCP.

Mechanical testing

All samples were tested at 25°C in the tensile mode on an Instron mechanical tester (model 4204) using a crosshead speed of 32 mm min^{-1}. An extensiometer (Instron model 2630-25) was used for all tests except for determination of the strength and elongation of neat PP. Strips of 10 mm × 76 mm were cut from the plaques and were sanded to minimize cutting marks. A minimum of five samples were tested and the average and standard deviation were calculated.

Scanning electron microscopy

Fracture surfaces of these materials were prepared by cryogenic fracture in liquid nitrogen followed by coating with gold in an SPI sputter coater. Fracture samples were viewed on a Cambridge Stereoscan S200 scanning electron microscope (SEM) using an accelerating voltage of 15 keV. Samples were taken from sprues, tensile bars and plaques. The sprues were fractured approximately 12 mm from the gate, at a sprue diameter of approximately

8 mm, and along the machine direction, so that the profile in the flow direction could be observed. Because of the narrow size in the neck section, the tensile bars were fractured only in the transverse direction. This fracture surface provides a machine-direction view of the dispersed phase. The plaques were fractured along the machine direction and, like the sprue samples, provide a flow-direction view. These plaque samples were subsequently etched in phosphoric acid as described by Olley *et al.*[33] for 15 min to better reveal the LCP morphology.

Contact-angle measurements

Contact angles of water, formamide and ethylene glycol on solid polymers were measured with a goniometer fitted with a video camera and monitor. These three liquids were chosen because of differences in their polar to dispersive components[34]. The solid polymer samples were prepared from injection-moulded plaques. These samples were cut from the plaques and rinsed with acetone prior to the measurement of contact angles. The contact angles of at least five drops per liquid were measured and averaged to determine the reported contact angle. These angles were determined with a standard deviation of approximately 2.8°.

Maleic anhydride interaction

The experimental methods used to determine if MAP reacted with the LCP are described in this section. In brief, PP(MAP) was extruded with and without LCPs to create test and control samples, respectively. Subsequently, the PP(MAP) was isolated from the LCP in test samples, and the relative change in the concentration of MAP between test and control was determined by means of *FT*i.r. spectroscopy.

In this investigation, a matrix rich in MAP (70 wt%) was used. One batch of this material was prepared by extrusion in a single-screw extruder at 250°C and 40 r.p.m., and it is referred to as the precursor. A neat sample of MAP would have been preferred, but there is insufficient melt strength for bringing strands of MAP to the pelletizer and hence some PP was included. The precursor was then dried overnight in a vacuum oven at 100°C while the LCP was dried overnight in a convection oven at 115°C. Control samples were prepared by extruding the precursor at approximately the same residence times and processing temperatures that would be used for preparation of the test samples. The test samples, or blends, were prepared by extrusion of the dried precursor with the LCP in a Killion single-screw extruder followed by pelletization. Blends of 30 wt % VA and VB were extruded with barrel zone temperatures of 125, 295 and 295°C, a die temperature of 200°C and a screw speed of 60 r.p.m. Blends of 30 wt% LC3000 were extruded with barrel zone temperatures of 125, 240 and 250°C, a die temperature of 200°C and a screw speed of 50 r.p.m.

Isolation of PP(MAP) from the control samples was accomplished by placing 10 g of the PP(MAP)/LCP blends in a flask with 250 ml of xylene. This suspension was agitated with a mechanical propeller under reflux for 3 h. Concurrently, a Büchner funnel was heated for several hours to 130°C in a convection oven. The PP(MAP)/LCP suspension was quickly filtered through the hot funnel, leaving primarily LCP as the extract and PP(MAP) as the filtrate. However, because the mixing process that occurs in the extruders can create fine submicrometre particles, filtrate samples from blends with VB and LC3000 possessed some LCP particles that could not be isolated from the PP(MAP) phase. The filtrate from the blends with VA possessed few if any of these particles. After filtration, approximately 30 ml of ethanol was added to the filtrate to precipitate the PP(MAP). This material was subsequently filtered and dried in a vacuum oven for three days at 100°C to isolate PP(MAP) from the solvents.

Samples of the isolated PP(MPA) were pressed to films of approximately 40 μm thickness at 200°C and dried in the vacuum oven at 100°C for three days prior to obtaining a *FT*i.r. spectrum. These spectra were obtained in a Nicolet FTIR, which was enclosed in a temporary dry-box to minimize the effects of moisture on the instrument. To average errors involved with measurement of film thickness, two spectra of each sample were taken at different locations on the film.

RESULTS AND DISCUSSION

The results of this work are organized along the following lines. First, the mechanical properties of these blends are presented as the concentration of MAP increases. Second, the morphology of these samples is observed in an attempt to relate the properties to the morphology. Third, the interfacial tension and work of adhesion are determined. This will establish if MAP also reduces interfacial tension and increases the work of adhesion, as commonly occurs for compatibilized TP blends. Finally, a discussion of the nature of the interaction between MAP and the LCPs will be presented.

Mechanical properties

The tensile strength of PP(MAP) with 30 wt% LCP is shown in *Figure 1* for tensile bars as the percentage of MAP within the PP(MAP) matrix rises to 50 wt%. The VA blend shows the least increase, from 44.5 to 55.1 MPa,

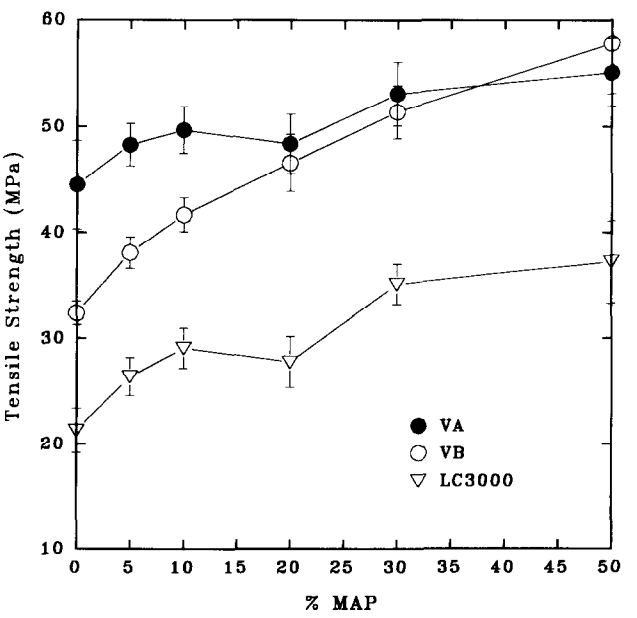

Figure 1 Tensile strength of 70 wt% PP(MAP) with 30 wt% LCP as the percentage of MAP in PP(MAP) increases from 0 to 50 wt%

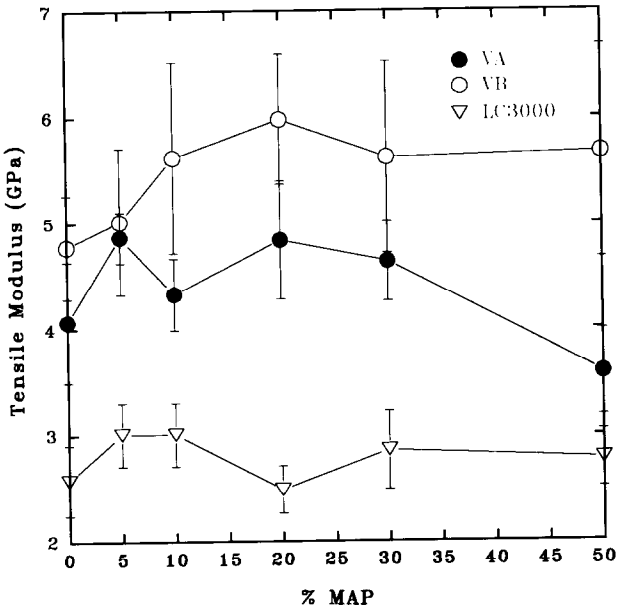

Figure 2 Tensile modulus of 70 wt% PP(MAP) with 30 wt% LCP as the percentage of MAP in PP(MAP) increases from 0 to 50 wt%

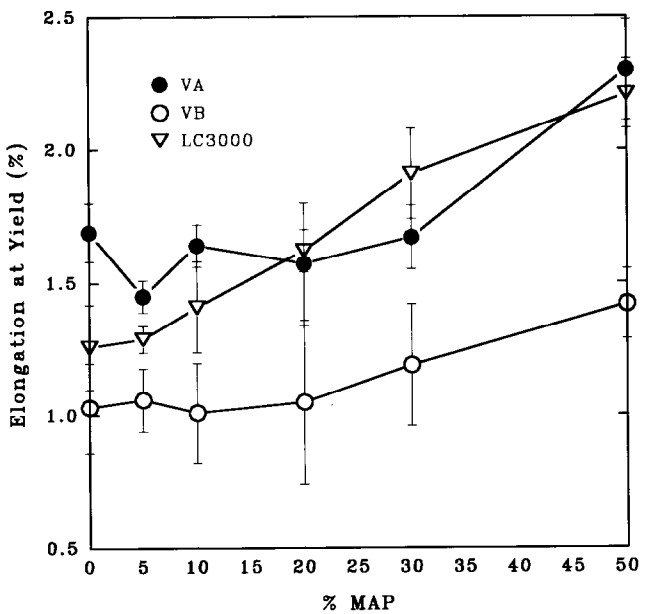

Figure 3 Elongation at yield of 70 wt% PP(MAP) with 30 wt% LCP as the percentage of MAP in PP(MAP) increases from 0 to 50 wt%

and this blend tends to display a plateau in the strength. The VB blend displays a large monotonic increase in strength without signs of reaching a plateau as the percentage of MAP increases to 50%. The strength of this blend increases from 32.4 to 57.8 MPa, a 78% increase, as the percentage of MAP increases from 0 to 50 wt%. Lastly, the strength of LC3000 increases from 21.3 to 37.2 MPa as the percentage of MAP increases from 0 to 50 wt%. It appears as in the case of VA blends that the tensile strength of the LC3000 blends may be reaching a plateau. However, higher concentrations of MAP would be required to determine accurately if a plateau exists.

The tensile modulus for these blends shows a less pronounced variation as the percentage of MAP increases as shown in *Figure 2*. For VA blends, there is an increase in the modulus from 4.07 to 4.67 GPa (with 90% statistical confidence) as the concentration of MAP is increased. However, the modulus for blends with 50% MAP decreases below that of the moduli of blends with 5 to 30% MAP. Blends with VB show a more pronounced increase in the modulus with the addition of MAP. The modulus increases from 4.8 GPa to a plateau of 5.7 GPa, a 19% rise with greater than 90% statistical confidence, at MAP concentrations higher than 5 wt%. For LC3000, there is no statistical change in the modulus with the addition of MAP.

The elongation at yield is also affected by the addition of MAP as shown in *Figure 3*. For VA blends, the elongation does not markedly change until 50 wt% MAP is added. It should be noted that this corresponds to the point where the modulus dropped. At 50 wt% MAP, the elongation is only 2.30%, half of the neat VA elongation, which is 4.35%. For VB blends, the elongation increases only at MAP percentages greater than 20%. However, at 50 wt% MAP the elongation, 1.42%, approaches the elongation of neat VB, which is 1.64%. The elongation of LC3000 blends displays a continual rise as the content of MAP increases. The highest elongation, which occurs at 50 wt% MAP, is 2.21%, and this value is slightly greater than the elongation of neat LC3000, which is 1.96%. This elongation is, however, much less than the elongation of neat PP (>9%), which indicates that LCP may be controlling the elongation. The elongation of the blend being slightly greater than the elongation of the neat LC3000 may be the result of higher LC3000 elongation in a less oriented state in the blend than in neat LC3000[35]. Overall, the approach of the blend elongation to the neat LCP elongation may indicate that the specimen is acting as an integral specimen instead of acting as a two-phase structure that can separate and fail prematurely.

The stress–strain curves of PP(MAP)/LCP tensile bars for three percentages of MAP are shown in *Figures 4* and *5*. The curves are composites of two or three actual stress–strain curves. The individual curves were selected to obtain close agreement with the average mechanical properties of the blend at the designated percentage of MAP. The stress–strain behaviour not only illustrates the changes in mechanical properties as a function of the percentage of MAP, but the curves may also indicate changes in adhesion and the mode of failure. It can be observed in *Figure 4* for blends of VA that the type of failure changes as the percentage of MAP increases. For both VA and VB blends, a transition from a ductile to a brittle failure occurs for samples with 50 wt% MAP. It is believed that the addition of MAP creates better adhesion between the LCP and PP[26,28,29]. Once the tensile stress or strain reaches the failure level of the LCP phase, which fails in a brittle mode, and the stress exceeds the strength of PP, failure of the blend occurs in a brittle fracture. This ductile to brittle transition and the mechanical property enhancements discussed above strongly suggest that adhesion between the phases is markedly improved. This transition does not occur with the LC3000 (*Figure 5*), but the lack of a ductile to brittle transition does not necessarily indicate that the compatibilizer is not effective with this LCP. Instead, it is

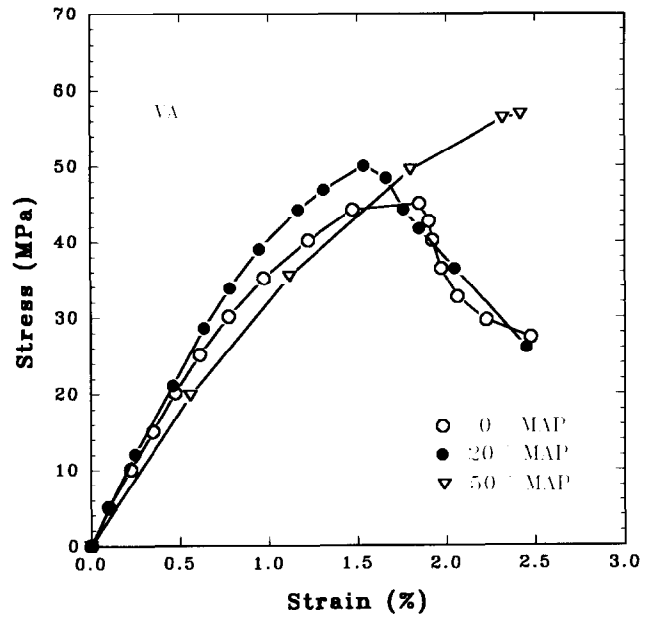

Figure 4 Stress–strain curves for 70 wt% PP(MAP) with 30 wt% VA as a function of the percentage of MAP

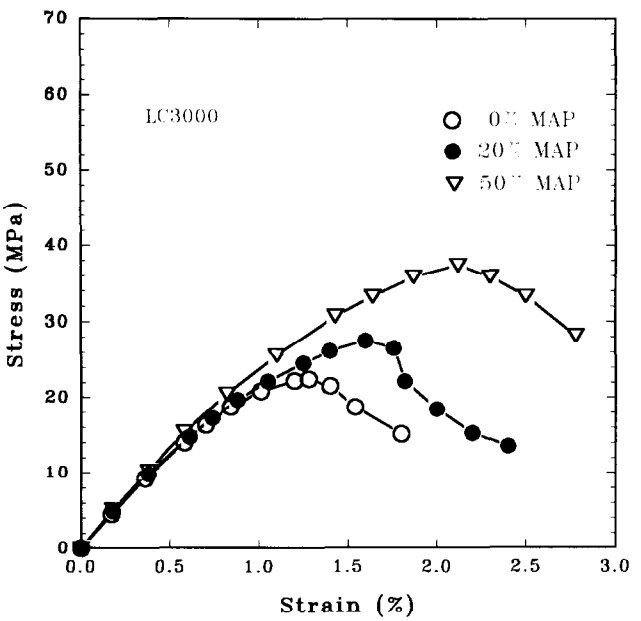

Figure 5 Stress–strain curves for 70 wt% PP(MAP) with 30 wt% LC3000 as a function of the percentage of MAP

possible that the stresses never significantly exceed the tensile strength of the PP phase, and so the PP still deforms in a ductile manner. Thus, in addition to improved mechanical properties, the incorporation of MAP into these blends can create a ductile to brittle transition. This transition may be indicative of markedly improved adhesion between the LCP and PP phases.

In the past, mechanical property differences between tensile bars and plaques were noted[26,28]. Examination of the mechanical properties of plaques can reveal information that differs from that of tensile bars. One difference is believed to be the result of the flow field present when the sample is moulded. Because of the converging region near the neck of the tensile bar, elongational flow exists, which can create high mechanical properties in neat LCPs[7,10]. However, the flow field in a plaque is predominantly that of a shear field, which creates less orientation and reinforcement than occurs in an extensional flow. The plaque is, however, reinforced by LCP that is deformed by flow in the advancing front. The flow in the advancing front is approximately an extensional flow field (hyperbolic stagnation flow)[36], and this flow field is responsible for the creation of a highly oriented skin region. Another primary difference between tensile bars and plaques is the ability to test the plaque specimens in both machine and transverse directions, whereas the tensile bar may only be tested in the machine direction. Accordingly, investigation of plaque properties can provide information about the anisotropy of the specimen. For compatibilized samples, measuring the mechanical properties in the transverse direction as the concentration of MAP increases indicates whether adhesion is improving. Testing in the transverse direction loads the sample in a series manner where the stress must pass from the matrix to the LCP. Consequently, the strength of the interface is tested more directly in the transverse direction than it is by performing tests on a sample in the machine direction.

The tensile properties of PP(MAP) and VA, VB, or LC3000 are shown in *Tables 1–3*, respectively. The common features are increases in tensile strength as the percentage of MAP increases. In the machine direction, the strength increases from 28.3 to 38.3 MPa for VA

Table 1 Tensile properties of PP/VA 70/30 plaques as affected by MAP content

MAP (%)	Strength (MPa)	Modulus (GPa)	Elongation at yield (%)
Machine direction			
0	28.3 (0.9)	2.96 (0.27)	1.51 (0.36)
5	31.6 (1.3)	3.07 (0.17)	1.57 (0.25)
10	31.9 (1.7)	2.90 (0.34)	1.70 (0.33)
20	35.8 (1.2)	2.78 (0.20)	1.74 (0.20)
30	39.3 (0.9)	3.02 (0.17)	1.69 (0.09)
Transverse direction			
0	12.0 (0.9)	1.41 (0.09)	2.57 (0.35)
5	12.8 (1.0)	1.26 (0.12)	2.54 (0.53)
10	13.9 (0.8)	1.43 (0.07)	2.63 (0.38)
20	15.6 (0.8)	1.18 (0.09)	2.90 (0.42)
30	16.7 (1.0)	1.57 (0.32)	2.37 (0.26)

Table 2 Tensile properties of PP/VB 70/30 plaques as affected by MAP content

MAP (%)	Strength (MPa)	Modulus (GPa)	Elongation at yield (%)
Machine direction			
0	23.1 (2.5)	3.69 (0.50)	1.04 (0.29)
5	25.3 (2.0)	3.99 (0.55)	0.96 (0.16)
10	28.3 (1.9)	4.15 (0.16)	1.04 (0.18)
20	36.7 (2.7)	4.20 (0.12)	1.14 (0.14)
30	40.3 (2.4)	4.94 (0.24)	0.97 (0.07)
Transverse direction			
0	11.8 (0.6)	1.54 (0.19)	1.54 (0.38)
5	12.3 (1.1)	1.60 (0.25)	1.95 (0.24)
10	14.6 (1.3)	1.58 (0.24)	2.01 (0.42)
20	16.9 (1.2)	1.61 (0.20)	1.50 (0.68)
30	17.8 (1.5)	1.71 (0.18)	1.44 (0.14)

Table 3 Tensile properties of PP/LC3000 70/30 plaques as affected by MAP content

MAP (%)	Strength (MPa)	Modulus (GPa)	Elongation at yield (%)
Machine direction			
0	14.4 (0.5)	1.81 (0.24)	1.15 (0.14)
5	18.6 (0.8)	2.07 (0.17)	1.27 (0.23)
10	23.5 (0.5)	2.30 (0.23)	1.64 (0.16)
20	20.2 (1.8)	2.33 (0.12)	1.53 (0.63)
30	26.2 (1.1)	2.18 (0.18)	1.94 (0.16)
Transverse direction			
0	7.6 (1.0)	1.28 (0.13)	0.73 (0.13)
5	10.0 (0.2)	1.25 (0.07)	0.97 (0.05)
10	13.3 (0.9)	1.34 (0.07)	1.23 (0.16)
20	11.8 (0.4)	1.18 (0.16)	1.23 (0.10)
30	16.1 (0.9)	1.29 (0.06)	1.71 (0.18)

blends, from 23.1 to 40.3 MPa for VB blends, and from 14.4 to 26.2 MPa for LC3000 blends. This increase in the strength of plaques follows similar increases in the strength of tensile bars. The strength also increases in the transverse direction as the percentage of MAP is increased. The strength increases from 12 to 16.7 MPa for VA blends, from 11.8 to 17.8 MPa for VB blends, and from 7.6 to 16.1 MPa for LC3000 blends. Since the strength of MAP, 30.6 MPa, is lower than the strength of PP, 36.7 MPa, the increases in the strength of the blends indicate that improved adhesion between the phases occurs with the addition of MAP.

Thus, MAP enhances the strength in both the machine and transverse directions of PP/LCP blends, while only the VB blends show a strong increase in machine-direction modulus with increasing MAP content. While the actual cause for the larger increase in machine-direction modulus for VB blends is not known, it is speculated that this increase in modulus is brought about either during formation of fibrils or through improved adhesion in the solid state as the result of the stronger hydrogen bonding that can be expected between MAP and VB[32]. The improvements in the transverse-direction strength of plaques with increasing MAP content in all three blends clearly indicates that MAP enhances the adhesion between PP and LCPs.

Morphology

It is anticipated that examination of the morphology of these blends will uncover relationships among the level of MAP, mechanical properties and structure of the blend. As mentioned in the 'Introduction', two limiting morphologies for TP/LCP blends have been observed: droplets and fibrils. At a fixed LCP concentration and with an increasing MAP concentration, it is of interest to determine if MAP changes the dispersed-phase size or

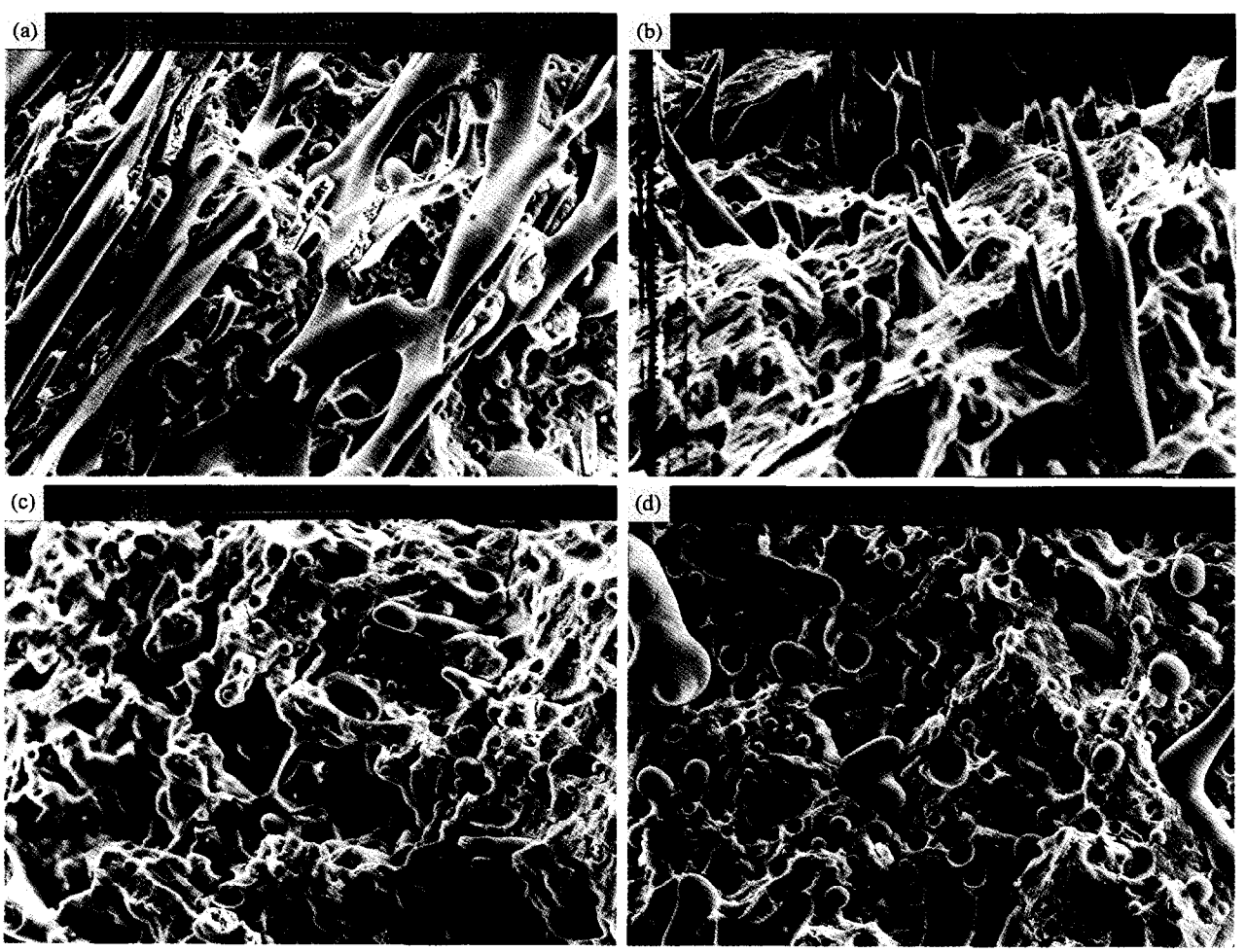

Figure 6 SEM micrographs of the core of a PP(MAP)/VA 70/30 sprue: (a) 5 wt% MAP; (b) 10 wt% MAP; (c) 20 wt% MAP; (d) 50 wt% MAP

shape. Accordingly, the morphology was investigated by examination of fracture surfaces from sprue, tensile bar and plaque samples.

The fracture surfaces of sprues from VA blends are shown in *Figures 6a–6d* for 5, 10, 20 and 50 wt% MAP, respectively. These views were centred near the core of the sprue where the temperature declined more slowly upon cooling and where more time for break-up of fibres into droplets existed before solidification occurred. In *Figure 6a*, the fracture surface of the VA blend with 5 wt% MAP is shown. A network-like system and micrometre-sized droplets exist simultaneously. It appears that some break-up via capillary instability may have been occurring when the material froze. At 10 wt% MAP, the network has nearly vanished, being replaced by long fibrils of approximately 10 μm. At 20 and 50 wt% MAP, the size reduction and dispersion of the LCP phase appears complete, with the formation of a droplet morphology. It must be pointed out that, since the centre of the sprue was not quickly quenched, it is not possible to state if this latter morphology is the direct result of a finer dispersion created before cessation of flow or if it is the result of a reduction in the phase size to the point where interfacial instabilities cause the break-up of the LCP before solidification occurs. In either case, the inclusion of MAP clearly causes a reduction in the phase size. Similar morphological changes are also observed for VB blends over this same composition range.

For LC3000 blends, while size reduction and increased dispersion occur with increasing concentration of MAP, numerous large sections of LC3000 exist at 10 and 20 wt% MAP. These large sections are finally dispersed at 50 wt% MAP. It has been found for PP/LC3000 blends that a viscosity ratio closer to unity leads to a finer dispersion, and as the percentage of MAP increases the viscosity ratio approaches unity[37].

Examination of the fracture surfaces in tensile bars illustrates the effect of MAP on the morphology in the neck region of the bar where an extensional flow may exist. *Figures 7a–7c* show the fracture surfaces for VA blends with 0, 20 and 50 wt% MAP, respectively. At 0 wt%, a coarse LCP structure exists, with a large distribution of sizes including ribbons and fibres. At 20 wt% MAP, the LCP phase becomes more uniform, with a fibrous appearance. The blend morphology becomes much finer and exhibits much smaller sizes at 50 wt% MAP. This was the concentration where the modulus decreased. It might be speculated that the aspect ratio of the LCP phase decreased with increasing MAP concentration. However, this information is not obtainable from this SEM, and the dogbone neck region was too small to permit fracture is a direction that would yield a view of the aspect ratio.

The same trends in morphological appearance exist for VB blends. It should be noted that, at 50 wt% MAP, the modulus of the VB blend does not decrease, and the

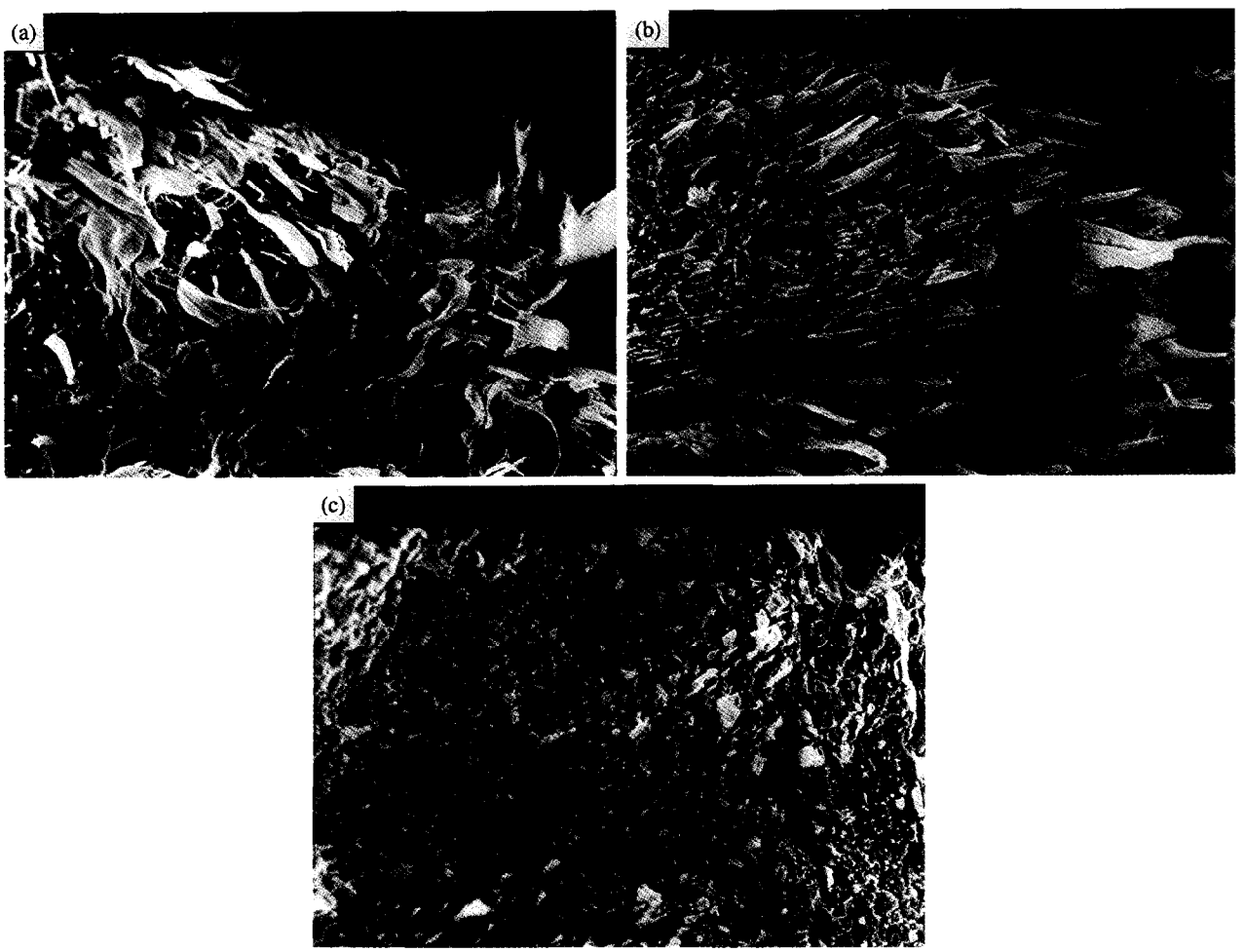

Figure 7 SEM micrographs of a PP(MAP)/VA 70/30 tensile bar: (a) 0 wt% MAP; (b) 20 wt% MAP; (c) 50 wt% MAP

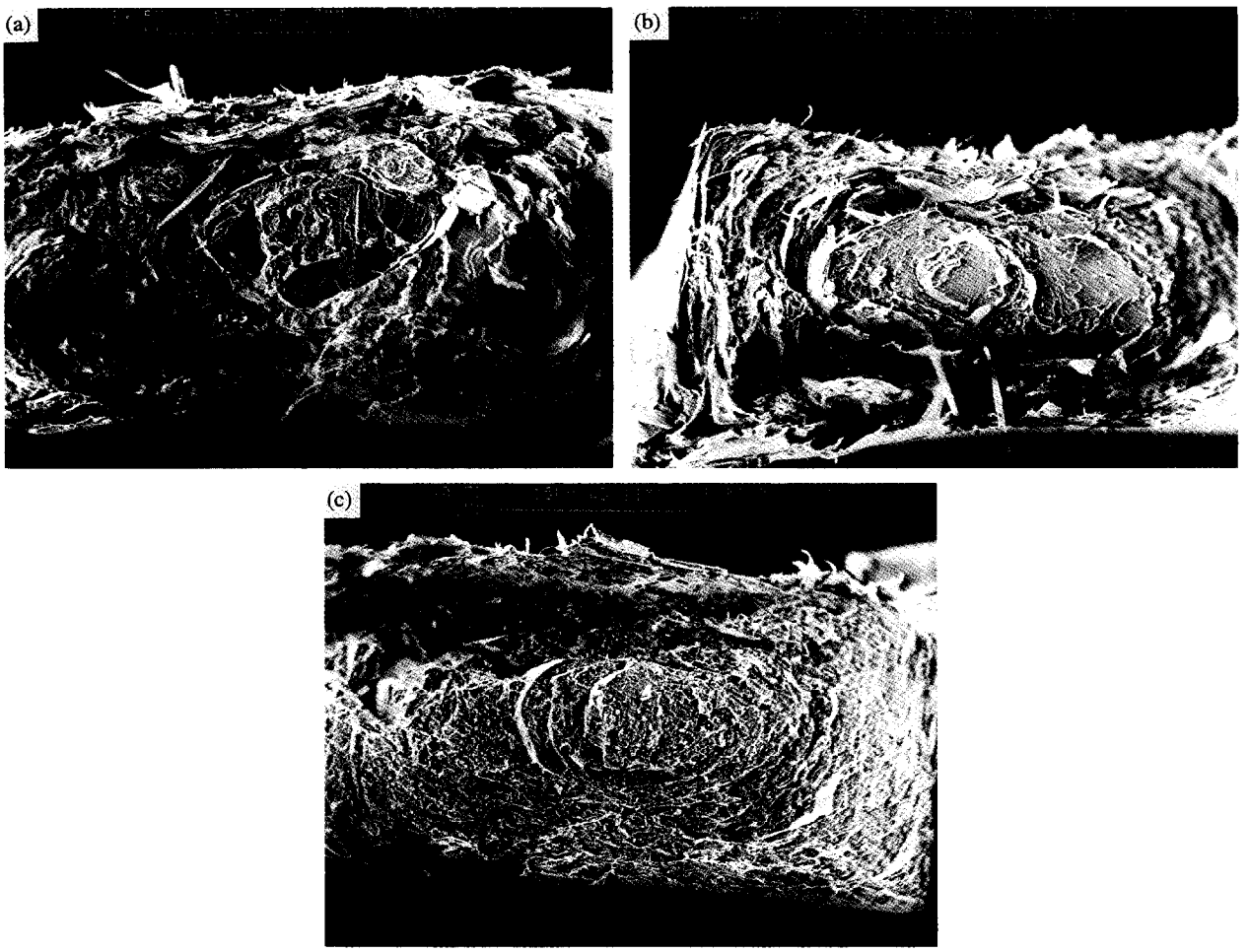

Figure 8 SEM micrographs of a PP(MAP)/LC3000 70/30 tensile bar: (a) 0 wt% MAP; (b) 20 wt% MAP; (c) 50 wt% MAP

morphology looks similar to the morphology of the VA blend, which exhibited the decreased modulus. It is probable that the aspect ratio of structures within the VA blend is reduced because of the additional MAP, while the aspect ratio of structures within the VB blend has not yet been sufficiently reduced to affect the modulus. Increasing the concentration of MAP beyond 50 wt% would be one means to determine if the modulus of VB blends would also drop.

In *Figures 8a–8c*, the fracture surfaces for the LC3000 blends with 0, 20 and 50 wt% MAP, respectively, are shown. Because of the large diversity in phase sizes, a much lower magnification is used in these photomicrographs (40 *versus* 180). It is suspected that the viscosity ratio, approximately 0.008, is too low to permit a fine dispersion of LC3000 in the PP(MAP) matrix. At 0 wt% MAP, little organization is observed in the LC3000 phase. It appears that more LCP is near the skin *versus* the core. At 20 wt% MAP, a pattern emerges as apparently more LCP is dispersed within the core of the tensile bar. Finally at 50 wt% MAP, a fine dispersion exists, with LC3000 evenly distributed throughout the sample. This concentration leads to the highest strength and elongation for the LC3000 blend. It is possible that, since more specific surface area exists for the dispersed blend, a higher amount of interaction on a volume basis exists, thus strengthening the blend.

Figure 9 illustrates the morphology of these blends within plaques. The fracture surfaces are along the machine direction, and both samples have been etched to reveal more of the LCP structure. The morphology of VA blends with 0 and 30 wt% MAP is shown in *Figures 9a* and *9b*, respectively. These photomicrographs are typical for all the blends studied. At 0 wt% MAP, a coarse structure is observed with a small ribbon-like morphology in the core, which gradually thickens as the skin is approached. A much finer structure is observed at 30 wt% MAP, with fine fibres in the core, which gradually change to thicker fibres and ribbons until only ribbons or films are observed near the skin. The reason for the progressive variation in the morphology is related to whether material experienced the fountain flow at the advancing front or whether the material experienced primarily shear flow. The presence of MAP in this plaque obviously acts to create a fine dispersion of LCP within the matrix. The VB and LC3000 morphologies are very similar to that of the VA blends and will not be shown here. It is obvious from these figures that MAP does act to disperse and reduce the size of the LCP phase. It also appears that eventually the aspect ratio can be decreased, leading to a reduction in properties.

Interfacial properties

Two of the three common characteristics of a compatibilizer are the reduction of interfacial tension and the improvement of adhesion between components

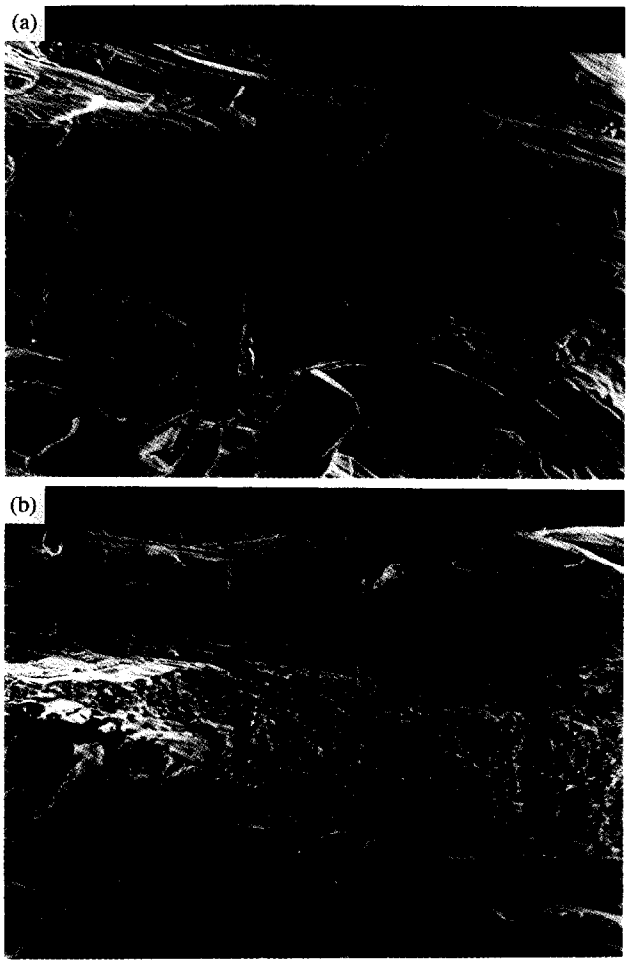

Figure 9 SEM micrographs of a PP(MAP)/VA 70/30 plaque: (a) 0 wt% MAP; (b) 30 wt% MAP

of a blend. These changes can be either measured or derived by various techniques. Often the interfacial tension for isotropic polymer melts can be measured by permitting an equilibrium between the two liquids to occur over the course of hours[38,39]. However, when working with two polymers that have marginally overlapping melt temperatures, equilibrium cannot be reached before significant degradation occurs. This is the situation for blends of PP with either VA or VB. Accordingly, an alternative technique that can be extrapolated to the melt is more suitable. Such a technique, which has been widely used, was proposed by Wu[40]. It consists of measuring the contact angle of two or more liquids on the surface of solid polymers. The liquids must have known polar and dispersive components of the surface tension. Then the contact angles and surface tensions may be used to determine the surface tension of the solid and from this the interfacial tension between polymers[28]. To perform this calculation, the contact angle of a liquid on a solid substrate is related to the surface and interfacial tension by a force balance. This relationship is known as Young's equation and is written as:

$$\gamma_{12} = \gamma_2 - \gamma_1 \cos\theta \tag{1}$$

where γ_{12} refers to the interfacial tension, and γ_1 and γ_2 refer to surface tension for the liquid and solid, respectively[41]. This equation is used in conjunction with the harmonic mean equation, which relates the interfacial tension to the polar and dispersive components of the surface tension for the liquid and solid[40,42]. This equation may be written as:

$$\gamma_{12} = \gamma_1 + \gamma_2 - 4\frac{\gamma_1^d \gamma_2^d}{\gamma_1^d + \gamma_2^d} - 4\frac{\gamma_1^p \gamma_2^p}{\gamma_1^p + \gamma_2^p} \tag{2}$$

where superscripts 'd' and 'p' designate the dispersive and polar components of the surface tension and their sum equals the surface tension, i.e. $\gamma = \gamma^d + \gamma^p$. A minimum of two liquids is required to find the polar and dispersive components of the solid surface tension. If more than two liquids are used, then a statistical fitting of the data is necessary. In this work, three liquids were used, and the above equations were solved using a non-linear least-squares fit. Once the interfacial tension at room temperature is calculated, these results may be extrapolated to the melt temperature using the average gradient of interfacial tension with respect to temperature as discussed by Wu[40]. Once having obtained the interfacial tension at room temperature, the work of adhesion may be calculated from:

$$W_a = \gamma_{s1} + \gamma_{s2} - \gamma_{12} \tag{3}$$

where 's' in the subscripts is a reminder that these are solid polymer surface tensions[41].

When using these techniques, it should be noted that there are some theoretical compromises or concerns. The first concern is that surface orientation of the plaques used for contact-angle measurements introduces some errors because the surface energies of oriented and unoriented surfaces differ for LCPs[43]. The second concern is that reactions may occur between the two polymers, especially with the use of a compatibilizer. If reactions at the interface occur, the contact-angle method would lead to overestimation of the interfacial tension.

With these potential shortcomings mentioned, the contact angles for PP, PP(MAP) with 10% MAP, and the three LCPs are listed in *Table 4*. In addition, the calculated surface tension and the dispersive surface tension percentage of these polymers are listed in the last two columns of *Table 4*. The three liquids used for determining the contact angles (water, formamide and ethylene glycol) were chosen because the range of dispersive surface tension percentages of these liquids (30 to 60%) improves statistical fitting of the data.

The calculated surface tension for PP is 25.6 mN m^{-1}. This compares favourably with the reported value[44] for PP of 29.4 mN m^{-1}. However, the dispersive component for PP should be approximately zero since this is an apolar polymer, and hence there is some discrepancy. The measurement of the dispersive component, 82% in this work, may be low as the result of additives in the PP. The introduction of 10 wt% MAP to PP increases the surface tension of the matrix by 1.4 mN m^{-1} and decreases the dispersive component. These trends would be expected for addition of a polar component to an apolar polymer. For the LCPs, the surface tension ranges between 34.9 and 40.4 mN m^{-1}. A value of 40.4 mN m^{-1} for LC3000 compares favourably to that of a common polyester, poly(ethylene terephthalate) (42.1 mN m^{-1})[40]. From the surface-tension data, the interfacial tension at

Table 4 Contact-angle data for neat polymers measured with water (θ_w), formamide (θ_f) and ethylene glycol (θ_e) and the resulting surface tension

Material	θ_w (deg)	θ_f (deg)	θ_e (deg)	γ (mN m^{-1})	$\gamma^d/\gamma \times 10^2$
PP	99.2 (4.6)	84.0 (2.6)	71.6	25.6	82.0
PP/BP 90/10	90.2 (3.9)	76.7 (3.3)	65.5	27.0	63.5
VA	78.0 (2.8)	56.4 (2.5)	52.7	34.9	54.6
VB	76.81 (3.2)	52.5 (1.4)	47.6	37.5	61.6
LC3000	67.1 (2.2)	49.3 (1.8)	46.2	40.4	46.3

Table 5 Interfacial tensions and work of adhesion for PP/LCP and PP(MAP)/LCP blends

	Interfacial tension (mN m^{-1})		Work of adhesion (mN m^{-1})	
	PP	PP/MAP	PP	PP/MAP
VA	6.3	1.5	54.2	60.4
VB	5.1	1.7	58.0	62.8
LC3000	11.2	4.5	54.8	62.9

room temperature may be calculated from the harmonic mean equation. Values of the calculated interfacial tension for PP and PP/MAP matrices are shown in *Table 5*. It is clear that the addition of 10 wt% MAP significantly lowers the interfacial tension.

In the previous section, it was shown that MAP reduces the phase size. Reduced interfacial tension and reduced phase size are consistent, since the size of a drop and its interfacial tension can be related through the critical Weber number[17]. This dimensionless number relates the hydrodynamic stress, $\eta\dot{\gamma}$, tending to deform and break a droplet, to the interfacial stress, γ_{12}/R. This ratio is typically written as $R\eta\dot{\gamma}/\gamma_{12}$, where R is the drop size, η is the viscosity, $\dot{\gamma}$ is the shear rate and γ_{12} is the interfacial tension. For a given shear rate and viscosity, a lowering of the interfacial tension would require that the drop size decrease to maintain the Weber number at a level where no further deformation occurs. Thus, the reduced phase size provides additional support for the claim that MAP reduces interfacial tension.

The work of adhesion, which is calculated from surface and interfacial tension, indicates that the presence of MAP increases the adhesion between the PP and LCP phases. As shown in *Table 5*, the addition of 10 wt% MAP increases the work of adhesion for all the blends. Using VB blends as an example, the work of adhesion increases 8.3% (58.0 to 62.8 mN m^{-1}) when the content of MAP increases from 0 to 10% MAP. Considering that, as the work of adhesion increases, fibre pull-out decreases[28,29] and tensile strength increases, the presence of MAP may enhance adhesion between the phases.

Thus, MAP in TP/LCP blends functions in a manner similar to a compatibilizer in TP blends, in that it leads to decreased interfacial tension, improved dispersion and enhanced adhesion. However, two distinct differences do exist. First, the morphology for TP/LCP blends must exhibit LCP structures with high aspect ratios to obtain reinforcement of the TP matrix. Second, instead of improving the impact strength and toughness, a compatibilizer for TP/LCP blends acts to improve the tensile properties of the blend. Thus, compatibilization of TP/LCP blends is similar to that of compatibilization of TP blends, but because high-aspect-ratio LCP structures are required for reinforcement, the morphology of *in situ* composites is drastically different from the droplet morphology of TP blends. This requirement apparently limits the amount of compatibilizer that can be used.

Interfacial reaction

The occurrence of a reaction or an interaction such as hydrogen bonding at the interface are two possible mechanisms to explain why MAP acts to enhance the mechanical properties of these blends. To distinguish between these two possibilities, comparison of the relative change in the maleic anhydride content in test and control samples was pursued. As discussed in the 'Experimental' section, a matrix consisting of PP(MAP) with 70 wt% MAP was prepared for the test and control samples. This material is referred to as the precursor. The control sample was prepared by re-extruding the precursor at the temperatures and residence time at which a test sample was prepared. The test sample was an extruded blend prepared from the precursor by adding 30 wt% LCP. Thus, the control sample separates the effect of time and temperature on maleic anhydride from the effect of reaction of maleic anhydride with the LCP that may occur in the test sample.

The relative amount of maleic anhydride in these samples was determined from *FT* i.r. spectra. It is well known that maleic anhydride displays a strong carbonyl absorption peak at 1784 cm^{-1}. Additionally, it is known that maleic anhydride is in equilibrium with its acids, maleic and fumaric. A shift in equilibrium to the acid form causes a shift in the carbonyl absorption from 1784 to 1714 cm^{-1}. Hence, drying the sample for three days is an important method to ensure formation of a large ratio of anhydride to acid functionalities.

Analysis of the change in the anhydride content from the precursor to the control samples was performed via two methods. The first method was to calculate the ratio of the area under the 1784 cm^{-1} absorption peak to the area under the 1220 cm^{-1} absorption peak, an internal reference that was reported as CH wag for PP[45]. This provides a relative concentration of maleic anhydride to PP in each of the samples. A ratio of this relative concentration for the control sample to the precursor sample thereby provides the percentage of maleic anhydride remaining in the control sample. The second method was to measure the peak height at 1784 cm^{-1} and the film thickness to obtain, via the Beer–Lambert law, the product of the extinction coefficient and the concentration. This latter method was also used between the test and control samples to obtain the percentage of maleic anhydride concentration remaining in the test sample. This method was employed because the presence of LCP particles in some test samples distorts the internal peaks needed for the internal reference method. Comparison of these methods shows that some discrepancy exists, and higher values were obtained from the internal reference method, i.e. 2 to 10% higher values.

Several reactions are possible within these blends. It is known that maleic anhydride-grafted PP can react with the amine ends of nylon-6[23]. While VB has an amine ingredient, *p*-aminophenol, it would be expected that the high reactivity of the amine would lead to their consumption prior to fully consuming the phenol. Thus, it is

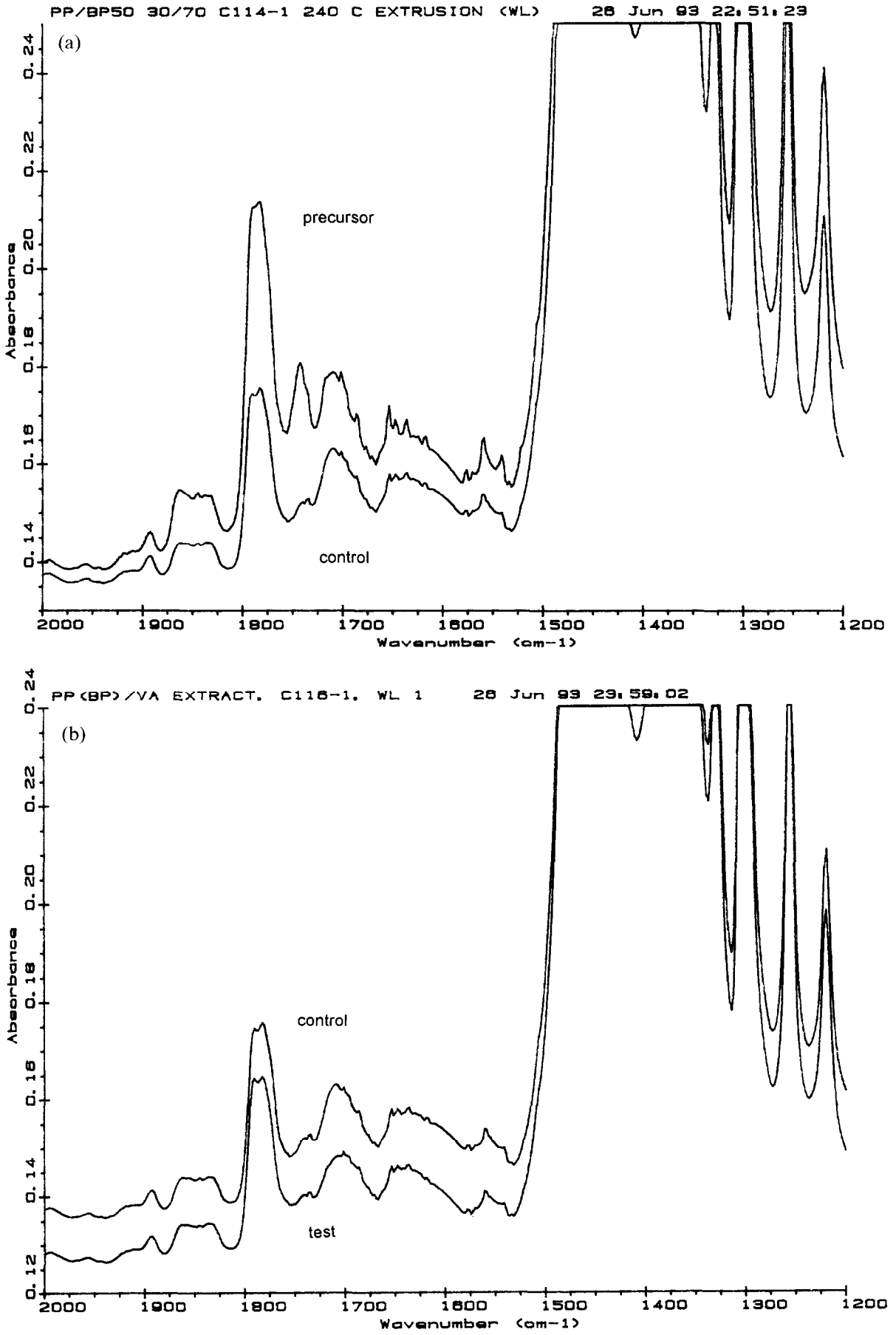

Figure 10 *FT* i.r. spectra for (a) precursor and control (extruded at 295°C), and (b) control (extruded at 295°C) and VA test samples

Table 6 Ratio of maleic anhydride content in extract to maleic anhydride content in precursor or control sample

	Melt temp. (°C)	Reference sample	Film thickness method	1220 cm^{-1} internal reference
PP/MAP	260	250°C precursor	84.9	87.0
PP/MAP	295	250°C precursor	55.9	67.7
PP(MAP)/VA	295	295°C control	99.2	106.0
PP(MAP)/VB	295	295°C control	98.7	n.a.
PP(MAP)/LC3000	250	260°C control	114.0	n.a.

doubtful that more than trace amounts of amine would exist in the LCP, so the amine ends would not be available for reaction with the maleic anhydride. Two of the LCPs are copolyesters, and reactions such as acidolysis might occur between the maleic anhydride and the ester moieties. However, this reaction usually requires catalysts to speed the reaction[46]. Thus, at least two types of reactions are possible, but for reasons outlined above they are not expected.

In *Table 6*, the relative changes of maleic anhydride content for control and test samples are reported. The melt temperature and the reference sample identification are listed as well as the residual percentage of maleic anhydride as determined by the two methods. Inspection of the first entry in *Table 6* shows the PP/MAP precursor was extruded to produce a control sample made at 260°C. This control sample shows a drop in the maleic anhydride content to 84.9 or 87.0% (film thickness and internal reference methods, respectively) *versus* the content found in the precursor. This percentage falls to 55.9 or 67.7% when the precursor was extruded at 295°C. The discrepancy between these methods was in the range of 2 to 10%, with the internal reference method always indicating a higher maleic anhydride content. Because of particles in the VB and LC3000 blends, only the thickness method could be used with these samples. However, few particles existed in the VA blend. Comparison of the spectra for the precursor and control samples (made at 295°C) and for the control and VA test samples is shown in *Figure 10*. In *Figure 10a*, the anhydride absorption at 1784 cm^{-1} for the control sample is clearly reduced from the anhydride absorption found in the precursor sample. In *Figure 10b*, there is no change in the anhydride absorption between the control and test samples. Also shown in *Figure 10a* is a change in the absorption at 1745 cm^{-1}. Although assignment for this wavenumber could not be found, this wavenumber is associated with PP and it indicates that PP is undergoing some change. However, no change at the reference wavenumber of 1220 cm^{-1} occurred, and it is believed that the internal reference method is valid.

It is clear from *Figure 10* and *Table 6* that both methods indicate that little if any maleic anhydride is consumed in blending MAP with VA. Instead, the change in maleic anhydride content results from degradation as indicated by comparison of the spectra of precursor and control samples. This conclusion can also be reached with the other two LCP blends. It should be mentioned that the > 100% residual maleic anhydride content in the LC3000 blend is believed to be the result of extruding the blend at a lower temperature than the temperature at which the control was made. The difference between extrusion temperatures of test and control samples occurred because of the poor operating performance of the test at the higher temperature. Thus, this work indicates that maleic anhydride does not react with LCP. However, since maleic anhydride degrades, it is possible that reactions between LCP and some of the degradation products occur, although this route seems doubtful.

CONCLUSIONS

The addition of MAP to the PP phase leads to significant mechanical property improvements in PP/LCP blends. The tensile strength for all three PP/LCP blends increases as the content of MAP is increased. A possible plateau in the tensile strength of VA blends occurs, and a decrease in the modulus occurs at the highest MAP concentration. This indicates that unlimited increase in the mechanical properties of these blends does not occur. However, significant increases in the strength can occur, and these increases are dependent upon the particular LCP. It does appear that the properties of the copoly(ester amide), VB, which can undergo strong hydrogen bonding, are strongly affected by the concentration of MAP. The tensile strength of this blend increases without limit in the range of MAP investigated, and the modulus shows large increases for both tensile bar and plaque specimens.

The addition of MAP to PP/LCP blends reveals increased dispersion of the LCP phase, reduced interfacial tension between the phases and enhanced adhesion, which are characteristics of compatibilized TP blends. However, differences exist between compatibilized TP blends and compatibilized TP/LCP blends. First, the use of MAP in these PP/LCP blends leads to improved tensile properties as opposed to improved impact strength and toughness observed in TP blends. Second, the addition of MAP to these blends leads to a finer dispersion of LCP within the matrix but with a more fibrillar structure being formed, which leads to reinforcement of the matrix. As shown by PP/VA blends, there is a point where mechanical properties diminish, and at this point the morphology appears to exhibit LCP structures with lower aspect ratios. Finally, it can be stated that maleic anhydride does not directly react with the LCP. Based on the significant enhancement of properties observed for PP/VB blends in the presence of MAP, it is believed that an interaction such as hydrogen bonding between MAP and LCP is the mechanism leading to the compatibilization of PP/LCP blends.

ACKNOWLEDGEMENTS

The authors would like to thank Joseph Humink of Uniroyal Inc. for supplying the development-grade maleic anhydride-grafted polypropylene. This work was supported by the Army Research Office (Grant Number DAAL03-91-G-0166), and their support is sincerely appreciated.

REFERENCES

1 Barham, P. J. and Keller, A. *J. Mater. Sci.* 1985, **20**, 2281
2 Done, D. and Baird, D. G. *Polym. Eng. Sci.* 1987, **27**(11), 816
3 Done, D. and Baird, D. G. *Polym. Eng. Sci.* 1990, **30**(16), 989
4 Kwolek, S. L., Morgan, P. W. and Schaefgen, J. R. in 'Encyclopedia of Polymer Science' (Ed. H. F. Mark), Wiley, New York, 1987
5 'Modern Plastics Encyclopedia', McGraw-Hill, New York, 1991
6 Lewis, D. N. and Fellers, J. F. in 'High Modulus Polymers' (Eds. A. Zachariades and R. S. Porter), Marcel Dekker, New York, 1988; p. 1
7 Ide, Y. and Ophir, Z. *Polym. Eng. Sci.* 1983, **23**(5), 261
8 Chung, T.-S. *J. Polym. Sci. (C) Polym. Lett.* 1986, **24**, 299
9 Chung, T.-S. *J. Polym. Sci. (B) Polym. Phys.* 1988, **26**, 1549
10 Kenig, S. *Polym. Eng. Sci.* 1987, **27**(12), 887
11 Kenig, S. *Polym. Eng. Sci.* 1989, **29**(16), 1136
12 Kohli, A., Chung, N. and Weiss, R. A. *Polym. Eng. Sci.* 1989, **29**(9), 573
13 Siegmann, A., Dagan, A. and Kenig, S. *Polymer* 1985, **26**, 1325
14 Nobile, M. R., Amendola, E. and Nicolais, L. *Polym. Eng. Sci.* 1989, **29**(4), 244
15 Blizard, K. G. and Baird, D. G. *Polym. Eng. Sci.* 1987, **27**(9), 653
16 La Mantia, F. P., Saiu, M., Valenza, A., Paci, M. and Magagnini, P. L. *Eur. Polym. J.* 1990, **26**(3), 323
17 Taylor, G. I. *Proc. R. Soc. (A)* 1934, **146**, 501
18 Tomotika, S. *Proc. R. Soc.* 1935, **150**, 322
19 Carfagna, C., Amendola, E., Nicolais, L., Acierno, D., Francescangeli, O. and Yang, B. *J. Appl. Polym. Sci.* 1991, **43**, 839
20 Blizard, K. G., Federici, C., Federico, O. and Chapoy, L. L. *Polym. Eng. Sci.* 1990, **30**(22), 1442
21 Zhuang, P., Kyu, T. and White, J. L. *Polym. Eng. Sci,* 1988, **28**(17), 1095
22 Meretz, S., Kwiatkowski, M. and Hinrichsen, G. *Int. J. Polym. Process.* 1991, **VI**, 239
23 Gaylord, N. G. *J. Macromol. Sci., Chem. (A)* 1989, **26**(8), 1211
24 Coran, A. Y. and Patel, R. *Rubber Chem. Technol.* 1983, **56**, 1045
25 Markham, R. L. *Adv. Polym. Technol.* 1990, **10**(3), 231
26 O'Donnell, H. J., Datta, A. and Baird, D. G. *SPE Tech. Pap.* 1992, **50**, 2248
27 O'Donnell, H. J., Chen, H. H. and Baird, D. G. *SPE Tech. Pap.* 1993, **51**, 1711
28 Datta, A., Chen, H. H. and Baird, D. G. *Polymer* 1993, **34**(4), 759
29 Datta, A. and Baird, D. G. *Polymer* 1995, **36**, 505
30 Heino, M. T. and Seppala, J. V. *J. Appl. Polym. Sci.* 1993, **47**, 1677
31 Jones, R. M. 'Mechanics of Composite Materials', Hemisphere, New York, 1975
32 East, A. J., Charbonneau, L. F. and Calundann, G. W. *Mol. Cryst. Liq. Cryst.* 1988, **157**, 615
33 Olley, R. H., Basset, D. C. and Bludell, D. J. *Polymer* 1986, **27**, 344
34 Kaelble, D. H., Dynes, P. J. and Cirlin, E. H. *J. Adhes.* 1974, **6**, 23
35 Acierno, D., La Mantia, F. P., Polizzotti, G., Ciferri, A. and Valenti, B. *Macromolecules* 1982, **15**(6), 1455
36 Tadmor, Z. *J. Appl. Polym. Sci.* 1974, **18**, 1753
37 O'Donnell, H. J. and Baird, D. G. *Int. J. Polym. Process.* in press
38 Anastasiadis, S. H., Gancarz, I. and Koberstein, J. T. *Macromolecules* 1988, **21**, 2980
39 Patterson, H. T., Hu, K. H. and Grindstaff, T. H. *J. Polym. Sci. (C)* 1971, **34**, 31
40 Wu, S. 'Polymer Interface and Adhesion', Marcel Dekker, New York, 1982
41 Adamson, A. W. 'Physical Chemistry of Surfaces', 4th Edn., Wiley, New York, 1982
42 Wu, S. *J. Polym. Sci. (C)* 1971, **34**, 19
43 Seeboth, A. M. *Angew. Makromol. Chem.* 1992, **196**, 101
44 Wu, S. in 'Polymer Handbook' (Eds. J. Brandrup and E. H. Immergut), Wiley Interscience, New York, 1989
45 Krim, S. *Adv. Polym. Sci.* 1960, **2**, 51
46 Kotliar, A. M. *J. Polym. Sci.: Macromol. Rev.* 1981, **16**, 367